Light Scattering Strategy for the Investigation of Time-Evolving Heterogeneous Supramolecular Self-Assemblies

Nicolas Jouault,[1,2] Emilie Moulin,[3] Nicolas Giuseppone,[3] and Eric Buhler[2,*]

[1]*Sorbonne Universités, UPMC Université Paris 06, CNRS, Laboratoire PHENIX, Case 51, 4 place Jussieu, F-75005 Paris, France*

[2]*Matière et Systèmes Complexes (MSC) Laboratory, UMR CNRS 7057, Sorbonne Paris Cité, University of Paris Diderot-Paris VII, Bâtiment Condorcet, 75205 Paris Cedex 13, France*

[3]*Université de Strasbourg, Institut Charles Sadron, CNRS, 23 rue du Loess, BP 84047, 67034 Strasbourg Cedex 2, France*

(Received 17 February 2015; published 19 August 2015)

Supramolecular self-assembly is a multiple length-scale and time-dependent process involving many coexisting components. Such complexity requires suitable strategies to extract quantitative dynamical and structural information on all involved species. Here, we detail an original light scattering method to study the kinetics of tailored triarylamine molecules capable of self-assembling in supramolecular highly conductive nanowires upon light exposure. These micrometric assemblies cause the emergence of intermittences in the scattered intensity and the construction of a predominant slow mode in the correlation function making separation between small-and large-size species impossible using conventional treatments. Our strategy is based on the time monitoring of intermittences and allows us to determine the fraction of nanowires as well as those of small critical nuclei and triarylamine building blocks as a function of time and light exposure, in good agreement with recent theoretical predictions.

DOI: 10.1103/PhysRevLett.115.085501 PACS numbers: 81.16.Dn, 82.70.Dd, 87.64.-t

Self-assembly of molecular building blocks through noncovalent associations offers the possibility of designing supramolecular responsive and adaptive ordered structures at the mesoscale with precise functions [1–4]. Hierarchical organizations can be triggered in solution by external stimuli (temperature, concentration, *p*H, light) to initiate the self-assembly from the molecular level to the macroscopic one. These directed processes create a certain number of coexisting components (i.e., building blocks, nonequilibrium intermediate assemblies, and final micrometric ordered structures) whose structural and dynamic behaviors have to be quantified with time. Depending on the supramolecular systems, multiple mechanisms have been proposed to explain the complex structural evolution with time and the final supramolecular morphology: nucleation-growth [5], sequential self-organization [6], competing behavior [7], cooperativity [8], or self-replication [9]. Understanding the kinetic self-assembly pathway may help to rationalize the design of materials in the desired shape and size [10].

Because of the multiple length-scale and time-dependent nature of these complex systems, experimental strategies have to be developed to characterize the composition of a mixed system and, in particular, the time-evolving behavior of all individual species. Several experimental techniques and methods (NMR spectroscopies or scattering techniques, among others) have been used to characterize such systems, but it still remains challenging to extract valuable information from the different components [11]. In this Letter, we propose an original experimental approach to quantitatively analyse complex time-evolving and large length-scale supramolecular systems using light scattering via the detection of intermittences in the scattered intensity temporal spectra associated with the formation of heterogeneous micrometric dense objects. To illustrate it, we conduct our method on tailored triarylamine (TAA) molecules capable of self-assembling in supramolecular highly conductive nanowires upon simple visible light exposure (Fig. 1) [12–17].

The origin of the supramolecular TAA nanowire (STANW) formation has been recently elucidated by a combination of experiments and theoretical tools [9] (Fig. 1). Light pulse induces the formation of radical

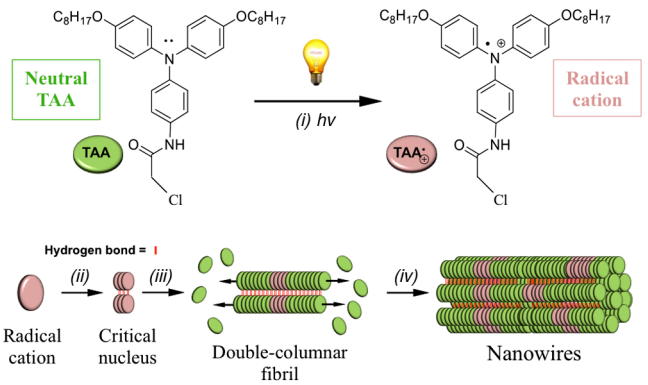

FIG. 1 (color online). Chemical structure of the tailored triarylamine (TAA) molecule used in experiments (upper left; chemical formula $C_{36}H_{49}ClN_2O_3$, and molecular weight of 593.25 g mol^{-1}), and schematic representation of the supramolecular self-assembly forming micrometric conducting nanowires obtained from the amine upon light irradiation.

cations $TAA^{\cdot+}$ necessary for the growth of the fibrillar structure and providing its autodoping. Radicals can aggregate with themselves and with neutral TAA by charge transfer in conjunction with hydrogen bonding, $\pi-\pi$ stacking, and dipole-dipole interactions. While TAA neutral molecules adopt a pyramidal conformation, radicals are flat and facilitate stacking. This coalition of interactions leads to the formation of molecular wires, which can combine into very strongly packed bundles of larger and stiffer micrometric fibrils. The radicals are a prerequisite for aggregation, and a solvent with oxidizing ability like chloroform is thus indispensable for the self-assembly, although the solvent itself does not induce oxidation of the TAA in the dark. $TAA^{\cdot+}$ Cl^- dipoles first aggregate to form double columns stabilized by significant lateral aggregation energy. The minimal stable double-columnar aggregate, called the critical nucleus, involves $n^*=3$ charge-transfer pairs per column: i.e., $2n^*=6$ dipoles, as predicted in Ref. [9]. Once such a critical nucleus is formed, it attracts neutral TAA molecules that attach at its ends by aromatic stacking and H bonding, thus initiating a proliferation of TAA aggregation without any further molecular oxidation. Critical nuclei formed by radicals are required for the self-assembly starting of neutral TAA. The nucleation stops before the reservoir of TAA is depleted, and for times $t \gg t_c$ (where $t_c = n^* t^*$) all fibrils should have roughly the same length. The nucleation stage (t^*) is always shorter than the growth stage (t_c). Also, the aggregation process turns out to be very fast in the case of light exposure for more than 5 s. Finally, this system shows sigmoid time dependency, suggesting a self-replicating behavior (i.e., the formation of the TAA self-assemblies facilitates its own formation).

Dynamic light scattering (DLS) is a powerful method allowing separation between small- and large-size species with relaxations widely separated in time and characterization of bimodal systems [18–22]. The physical origin of fast and slow modes may differ according to the system considered. In particular, diffusion of large particle aggregates [20], relaxation of charge fluctuations [21], viscoelastic processes [22], slow fluctuations in nonergodic systems such as glasses or gels [23,24], or multiple light scattering in turbid media [25] are possible mechanisms that might be responsible for a slow component in the correlation function and have led to seminal DLS developments. In dilute equilibrium systems, fluctuations in the scattered intensity with time, $I(q,t)$, measured at a given scattering angle θ or, equivalently, at a given scattering wave vector $q=(4\pi n/\lambda)\sin(\theta/2)$, are directly reflecting the so-called Brownian motion of the scattering particles. However, for very heterogeneous systems—i.e., with a large-size distribution—or systems having fast-evolving structures such as our studied one, micrometric objects behave as dust going randomly through the laser beam, causing the appearance of intermittences in the count rate and the construction of a slow mode of large amplitude in the correlation function, making the analysis of the fast relaxation processes of the greatest interest impossible. To overcome this issue, we propose a quantitative method for extracting information on small objects, as the TAA critical nuclei whose proportion may evolve with time and whose contribution in the short time range of the correlation function is masked by the slow contribution associated with the formation of micrometric aggregates (here, the STANWs). Also, it was not possible to characterize the critical nuclei of a few nanometers, and their evolution with time during the aggregation process with neutron or x-ray scattering as the signal is dominated by the STANWs and the acquisition time is much larger than the kinetic characteristic times.

Solution of TAA in chloroform is light yellow right after purification. It proved stable for a long time if kept in the dark. When exposed to visible light with a 20 W power lamp, it changes color to light green. These changes persist for a few weeks in the dark and are attributed to the self-assembly of TAA [12]. Dilute solutions of monomeric TAA [7.5 mM (0.45 vol%)] were prepared in deuterated chloroform $CDCl_3$. Dust and impurities were removed from the samples before irradiation by filtration through 0.22 μm PTFE Millipore filters. Prior to irradiation with visible light, no evidence for the presence of self-assemblies or larger objects could be deduced in DLS since no characteristic decays were observed in the intensity correlation function. The relaxation associated with the diffusion of free diluted small TAA molecules in chloroform is too fast to be detected in the short time range of the correlation function.

First, the evolution of the size of the scattered objects has been probed after different pulses of light irradiation (5, 10, and 15 s) for the first time in this study. Small-size species could be characterized as soon as the amplitude of the STANW's slow mode is not predominant. Figure 2(a) shows the evolution of the normalized time intensity autocorrelation function [Eq. (1)], measured with homodyne scattering experiments at a scattering angle θ of 90° over 1 h in the dark of TAA solution lightened for 5 s prior to measurement:

$$\frac{g^{(2)}(q,t)-g^{(2)}(q,\infty)}{g^{(2)}(q,0)-g^{(2)}(q,\infty)}=|g^{(1)}(q,t)|^2. \qquad (1)$$

The correlation function is clearly bimodal and can be described by the sum of two exponential decays superposed with an oscillatory term. The well-defined oscillations, independent of the scattering wave vector q, measured in the long time range are caused by convection due to the local heating of the highly absorbing sample by the incident laser beam [26]. The two exponential decays are deconvoluted using the CONTIN program to yield the amplitudes of the two modes as well as hydrodynamic radii R_h associated with the two relaxations (see the Supplemental Material [27] for details). The insert shows the distribution of the scattered intensity with R_h obtained by applying the CONTIN analysis to the data compiled between 10^{-6} and

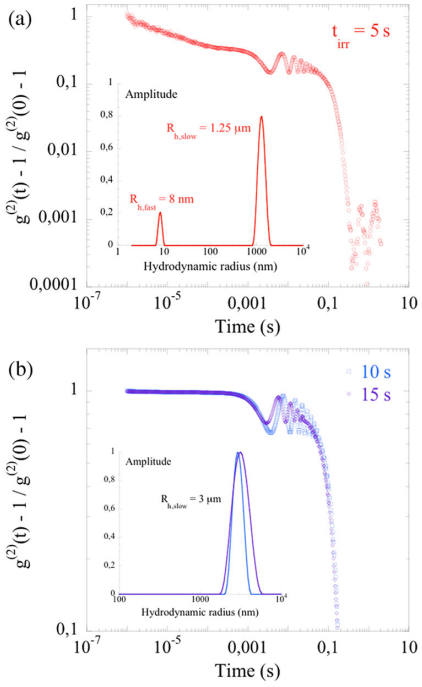

FIG. 2 (color online). Evolution with irradiation time of the intensity correlation function averaged over one hour for a 7.5 mM TAA solution at $\theta = 90°$. (a) 5 s of irradiation. (b) 10 and 15 s of irradiation. The inset shows the normalized distribution of the scattered intensity with the size by applying the CONTIN analysis between 10^{-6} and 2×10^{-3} s.

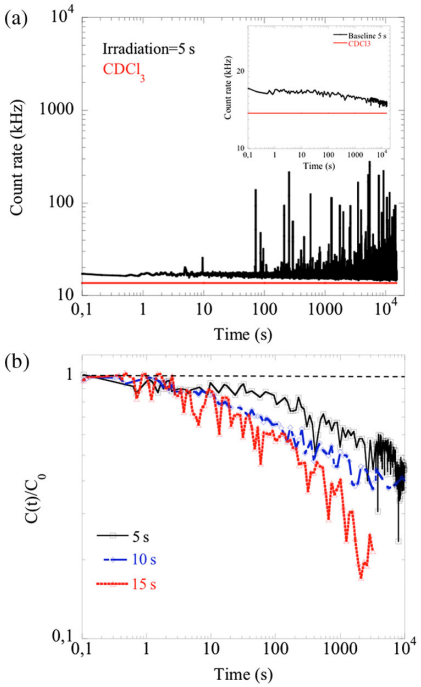

FIG. 3 (color online). (a) Evolution with time of the scattered intensity (count rate in kHz) at a scattering angle of 90° for a 7.5 mM solution of TAA molecules in chloroform illuminated for 5 s. The insert shows the evolution of the baseline count rate over time. The red line corresponds to the count rate of pure chloroform. (b) $C(t)/C_0$ evolution over time after 5 s (black squares), 10 s (blue diamonds), and 15 s (red triangles) of light irradiation.

2×10^{-3} s; i.e., the long time range oscillatory relaxation is not included in this analysis. One found $R_h = 8$ nm for the fast diffusive decay associated with small self-assemblies defined as critical nuclei with $n^* > 2$ [9], and characterized here for the first time. As deduced from the presence of a second slow process in the correlation function, the samples contain a second class of particles about 2 orders of magnitude larger than the small assemblies. The value of 1.25 μm is larger than the experimental length scale q^{-1} of 300 nm, but it gives a good order of magnitude for the dense fibrillar nanowire aggregates described above [28]. These micrometric fibers can also be seen with the naked eye as they glitter in the laser beam and are responsible for intermittences in the scattered intensity temporal spectra. TAA molecules self-assemble into two thermodynamically stable structures, a large one corresponding to the nanowires and one smaller in size corresponding to critical nuclei.

Interestingly, for longer light irradiation times [10 and 15 s; see Fig. 2(b)], the amplitude of the slow mode, A_{slow}, is increased and reaches a value close to 100%, which makes analysis of the fast contribution associated with the critical nuclei impossible, as the slow mode totally masks the 8 nm critical nuclei relaxation in the short time range of the correlation function and indicates that the mass and/or the number of micrometric fibers have been increased. However, critical nuclei, from which columnar fibrils grow by supramolecular association of neutral TAA, are in large numbers at the beginning of the kinetic and their evolution with time and their irradiation time is of significant importance. Their number is expected to drop rapidly during the growth process, and for this reason a different method is proposed for having access to such kinetic properties and to their concentration over the whole time span of the aggregation process. For that purpose the count rate [i.e., the intensity-time curve $I(t)$] has been monitored over four hours after irradiation at a scattered angle of 90°.

Figure 3(a) and its insert display the count rate and the evolution of its baseline as a function of time in the dark after 5 s of light irradiation, respectively. Around 70 s after the counting starts, extra-high jumps in the $I(t)$ curve (peaks with intensity larger than 100 kHz) due to the formation of large aggregates are intermittently observed, giving a real time display of STANWs passing through the laser beam. The amplitude is directly correlated to the mass of the STANWs: the higher the amplitude, the higher the mass (typical size $d > 1$ μm and scattered intensity $I \approx d^6$). One notes that, for 5 s of light irradiation, the maximal amplitude is around 300 kHz, while it reaches 5000 kHz for 10 and 15 s (see the Supplemental Material [27]), indicating that larger objects are formed with longer light exposure. This experiment shows that the first micron size object (i.e., the first peak) appears ≈70 s after the counting rate measurement starts—that is, 70 s after irradiation; this appearance time is shortened to ≈15 s if the irradiation time is increased to 15 s (see the Supplemental Material [27]).

The count rate baseline represents the fluctuations of scattered intensity associated with the fast process observed in Fig. 2, i.e., with the total scattered intensity reduced by intermittent count rates jumping associated with the micrometric supramolecular fibers. The baseline level is thus directly related to the concentration of critical nuclei made of six $TAA^{\cdot+}$, and of free $TAA^{\cdot+}$ and neutral TAA (which are too small to display a relaxation in the correlation function) and decreases with time until almost reaching the intensity of pure chloroform for infinite times, indicating that TAA and nuclei are consumed during the polymerization process. Note that, when the light irradiation is switched off, the amounts of radicals decrease like $1/t$ to reform neutral TAA [9]. The Rayleigh ratio (see the Supplemental Material [27]) at $t = 0$, when fibers are not formed, gives an estimate of the TAA and critical nuclei amounts as $R_{t=0} = K.(C_{\text{free TAA}}.M_{\text{TAA}} + C_{\text{free TAA}^{\cdot+}}.M_{\text{TAA}^{\cdot+}} + C_{\text{nuclei}}.M_{\text{nuclei}})$, where K is the scattering constant (see the Supplemental Material [27]). According to our previous study, the mass of the critical nuclei is constant with time and equal to that of six TAA molecules, i.e., of $2n^*$ dipoles ($M_{2n*} = M_{\text{nuclei}} = 6M_{\text{TAA}} = 3559.5\,\text{g mol}^{-1}$) [9]. With $C_{\text{total}} = C(t=0)_{\text{free TAA}} + C(t=0)_{\text{free TAA}^{\cdot+}} + C_{\text{nuclei}}(t=0)$, one finds $C(t=0)_{\text{free TAA+TAA}^{\cdot+}} = 4\times10^{-3}\,\text{g/cm}^3$ and $C_{\text{nuclei}}(t=0) = 4.5\times10^{-4}\ \text{g/cm}^3$, for an irradiation of 5 s. The nuclei amount is found to be quite similar for 10 and 15 s irradiation times; however, the concentration of free radicals that could not be determined with these experiments should depend on the illumination rate.

To understand the nanowires formation, we then followed the evolution of the free TAA and critical nuclei concentration with time since this information is contained in the count rate baseline level. Neglecting the virial effects and considering that the nuclei form factor tends to 1 (an assumption comforted by the value of $R_{h,\text{critical nuclei}} \approx 8$ nm that is smaller than 30 nm, i.e., the limit measurable size in static light scattering), the baseline intensity can be expressed as

$$\begin{aligned} I_{\text{baseline}}(q,t) &\approx C_{\text{free TAA}}(t)M_{\text{TAA}} + C_{\text{free TAA}^{\cdot+}}(t)M_{\text{TAA}} \\ &\quad + C_{\text{nuclei}}(t)M_{\text{nuclei}} \\ &= [C_{\text{free TAA}}(t) + C_{\text{free TAA}^{\cdot+}}(t) \\ &\quad + 6C_{\text{nuclei}}(t)]M_{\text{TAA}}, \end{aligned} \tag{2}$$

where $C_{\text{free TAA}}(t)$, $C_{\text{free TAA}^{\cdot+}}(t)$ and $C_{\text{nuclei}}(t)$ represent concentrations at time t of free neutral TAA, of free radicals, and of the nuclei, respectively. Finally, for the $I(t)/I_0$ ratio, one obtains

$$\frac{I(t)}{I_0} = \frac{C_{\text{free TAA}}(t) + C_{\text{free TAA}^{\cdot+}}(t) + 6C_{\text{nuclei}}(t)}{C_{\text{free TAA}}(0) + C_{\text{free TAA}^{\cdot+}}(0) + 6C_{\text{nuclei}}(0)} = \frac{C(t)}{C_0}. \tag{3}$$

Experimentally, $I(t)$ represents the ratio $(I_{\text{baseline}} - I_{\text{CDCl}_3})/I_{\text{toluene}}$, where I_{toluene} and I_{CDCl_3} are the measured scattering intensities of reference toluene and deuterated chloroform [the red line in Fig. 3(a)], respectively. Figure 3(b) shows the $C(t)/C_0$ evolution with time after different irradiation times (5, 10, and 15 s). We observe that $C(t)/C_0$ decreases over the whole experiment time, revealing that there are almost no remaining free nuclei and TAA after 4 h in the dark for 15 s of light exposure. The decay rate of the $C(t)/C_0$ curve is also clearly stronger when the irradiation time is increased. These results confirm previous works indicating that primary TAA and critical nuclei are consumed to form micrometric fibrils. Since these fibrils do not contribute to the count rate baseline, one can deduce their time-dependent fraction $w(t)$, which corresponds to $\approx 1 - C(t)/C_0$ (Fig. 4). For all irradiation times, $w(t)$ shows a sigmoid evolution—i.e., a low fraction regime at short time followed by an increase more or less pronounced and by a plateau at infinite time—expressed as $w(t) = K\tanh(tn^*/t_c)$ [9], where K represents the fibrils self-assembly rate, which should be equal to 1 if the solution is composed of 100% fibrils at infinite time. We have to point out that these predictions have been made for samples continuously exposed to light during 1 h, i.e., having a high proportion of critical nuclei initiating the fibrils formation and the TAA consumption. Therefore, our data have been fitted using a similar expression, $K\tanh(tn^*/t_c)^{\alpha}$, in which a stretched exponent $\alpha = 1/3$ has been used to take into account the lower steepness of the experimental sigmoidlike variations due to the short experimental irradiation times and to the relaxation of free radicals in $1/t$ after illumination switch-off [9]. From the best fits of the data shown in Fig. 4, one obtains growth times $t_c = 18574$, 1908, and 1862 s and $K = 0.58$, 0.60, and 0.74 for irradiation times of 5, 10, and 15 s, respectively. As expected, the growth characteristic time t_c decreases with the irradiation time while K increases, showing that the concentration of small units has become pretty low, in good agreement with theoretical predictions.

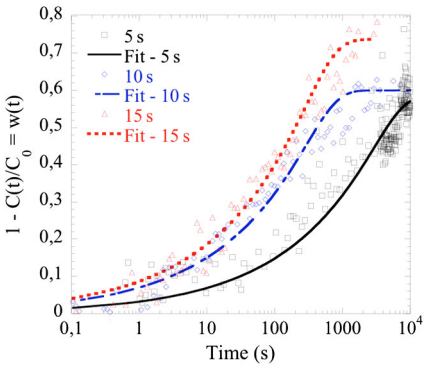

FIG. 4 (color online). $1 - C(t)/C_0$ evolution with time for the different irradiation times: 5 s (black squares), 10 s (blue diamonds), and 15 s (red triangles). The lines correspond to the best fits of the data (see the main text).

To summarize, the time monitoring of intermittences allows us to follow the formation of micrometric nanowires

in a light-induced time-evolving heterogeneous supramolecular system. Our results give the time-dependent concentrations of all species of very different sizes and allow the characterization of the complex overlap between nucleation-growth and self-replicating processes in this system. The presence of large heterogeneous species such as aggregates leading to the emergence of intermittences and of a slow mode of very large amplitude ($A_{slow} \approx 100\%$) masking the contribution of small units in the short time range of the correlation function is a common experimental situation encountered in many aggregating systems. One may thus predict that our method can be applied to a variety of studies involving other types of complex, colloidal, or biological systems having multiple components in large length and time scales—such as functional organic materials [29–34], protein fibrils, polymer or micellar solutions [35,36], nanofluids [37], or giant viruses and bacteria-drug systems [38,39]—covering a wide range of applications in materials as well as in the biological sciences.

The research leading to these results has received funding from the European Research Council under the European Community's Seventh Framework Program (FP7/2007–2013) / ERC Starting Grant Agreement No. 257099 (N. G.). This work was also supported by a postdoctoral fellowship (N. J.) from the Agence Nationale de la Recherche (No. ANR-09-BLAN-034-02).

*eric.buhler@univ-paris-diderot.fr

[1] L. Brunsveld, B. Folmer, E. Meijer, and R. Sijbesma, Chem. Rev. **101**, 4071 (2001).
[2] B. Rybtchinski, ACS Nano **5**, 6791 (2011).
[3] E. Busseron, Y. Ruff, E. Moulin, and N. Giuseppone, Nanoscale **5**, 7098 (2013).
[4] J. M. Lehn, Angew. Chem., Int. Ed. **52**, 2836 (2013).
[5] J. Elemans, A. E. Rowan, and R. J. M. Nolte, J. Mater. Chem. **13**, 2661 (2003).
[6] M. Ruben, U. Ziener, J. M. Lehn, V. Ksenofontov, P. Gutlich, and G. B. M. Vaughan, Chem. Eur. J. **11**, 94 (2005).
[7] M. Bellot and L. Bouteiller, Langmuir **24**, 14176 (2008).
[8] P. Besenius, G. Portale, P. H. H. Bomans, H. M. Janssen, A. R. A. Palmans, and E. W. Meijer, Proc. Natl. Acad. Sci. U.S.A. **107**, 17888 (2010).
[9] I. Nyrkova, E. Moulin, J. J. Armao, M. Maaloum, B. Heinrich, M. Rawiso, F. Niess, J. Cid, N. Jouault, E. Buhler, A. N. Semenov, and N. Giuseppone, ACS Nano **8**, 10111 (2014).
[10] P. A. Korevaar, C. Grenier, A. J. Markvoort, A. Schenning, T. F. A. de Greef, and E. W. Meijer, Proc. Natl. Acad. Sci. U.S.A. **110**, 17205 (2013).
[11] M. C. Misuraca, E. Moulin, Y. Ruff, and N. Giuseppone, New J. Chem. **38**, 3336 (2014).
[12] E. Moulin, F. Niess, M. Maaloum, E. Buhler, I. Nyrkova, and N. Giuseppone, Angew. Chem., Int. Ed. **49**, 6974 (2010).
[13] V. Faramarzi, F. Niess, E. Moulin, M. Maaloum, J. F. Dayen, J. B. Beaufrand, S. Zanettini, B. Doudin, and N. Giuseppone, Nat. Chem. **4**, 485 (2012).
[14] E. Moulin, J. J. Cid, and N. Giuseppone, Adv. Mater. **25**, 477 (2013).
[15] J. J. Armao, M. Maaloum, T. Ellis, G. Fuks, M. Rawiso, E. Moulin, and N. Giuseppone, J. Am. Chem. Soc. **136**, 11382 (2014).
[16] Y. Domoto, E. Busseron, M. Maaloum, E. Moulin, and N. Giuseppone, Chem. Eur. J. **21**, 1938 (2015).
[17] E. Busseron, J.-J. Cid, A. Wolf, G. Du, E. Moulin, G. Fuks, M. Maaloum, P. Polavarapu, A. Ruff, A.-K. Saur, S. Ludwigs, and N. Giuseppone, ACS Nano **9**, 2760 (2015).
[18] W. Schärtl, *Light Scattering from Polymer Solutions and Nanoparticle Dispersions* (Springer, New York, 2007).
[19] *Photon Correlation and Light Beating Spectroscopy*, edited by H. Cummins, Nato Science Series B Vol. 3 (Springer, New York, 1974).
[20] N. Jouault, Y. J. Xiang, E. Moulin, G. Fuks, N. Giuseppone, and E. Buhler, Phys. Chem. Chem. Phys. **14**, 5718 (2012).
[21] J. Appell, G. Porte, and E. Buhler, J. Phys. Chem. B **109**, 13186 (2005).
[22] E. Buhler, J. P. Munch, and S. J. Candau, Europhys. Lett. **34**, 251 (1996).
[23] J. Müller and T. Palberg, Prog. Colloid Polym. Sci. **100**, 121 (1996).
[24] P. Pusey and W. van Megen, Physica (Amsterdam) **157A**, 705 (1989).
[25] M. Heckmeier and G. Maret, Prog. Colloid Polym. Sci. **104**, 12 (1997).
[26] The analytical treatment and a new theory explaining this behavior as arising from the heterodyning of scattered light from two distinct species will be presented in a forthcoming study.
[27] See Supplemental Material at http://link.aps.org/supplemental/10.1103/PhysRevLett.115.085501 for light scattering methods; evolution with time of the count rate for TAA solutions illuminated for 5, 10, and 15 s.
[28] The slow process being superposed with an oscillatory term, this value could be truncated.
[29] P. A. Korevaar, S. J. George, A. J. Markvoort, M. M. J. Smulders, P. A. J. Hilbers, A. P. H. J. Schenning, T. F. A. De Greef, and E. W. Meijer, Nature (London) **481**, 492 (2012).
[30] J. Kang, S. Miyajima, T. Mori, Y. Inoue, Y. Itoh, and T. Aida, Science **347**, 646 (2015).
[31] S. Ogi, V. Stepanenko, K. Sugiyasu, M. Takeuchi, and F. Würthner, J. Am. Chem. Soc. **137**, 3300 (2015).
[32] S. Ogi, K. Sugiyasu, S. Manna, S. Samitsu, and M. Takeuchi, Nat. Chem. **6**, 188 (2014).
[33] N. Javid, S. Roy, M. Zelzer, Z. Yang, J. Sefcik, and R. V. Ulijn, Biomacromolecules **14**, 4368 (2013).
[34] J. Boekhoven, J. M. Poolman, C. Maity, F. Li, L. van der Mee, C. B. Minkenberg, E. Mendes, J. H. van Esch, and R. Eelkema, Nat. Chem. **5**, 433 (2013).
[35] M. Kanao, Y. Matsuda, and T. Sato, Macromolecules **36**, 2093 (2003).
[36] K. Morishima and T. Sato, Langmuir **30**, 11513 (2014).
[37] R. Prasher, P. Phelan, and P. Bhattacharya, Nano Lett. **6**, 1529 (2006).
[38] J. Perlmutter and M. Hagan, Annu. Rev. Phys. Chem. **66**, 217 (2015).
[39] N. Philippe *et al.*, Science **341**, 281 (2013).